



# Structural Analysis of Unsymmetric Laminated Composite Timoshenko Beam Subjected to Moving Load

Mohammad Javad Rezvani

*Department of Mechanical Engineering, Semnan Branch, Islamic Azad University, Semnan, 35145-179, Iran*

*\*Corresponding Author: m.rezvani@semnaniau.ac.ir*

**(Manuscript Received --- 05, 2017; Revised --- 10, 2017; Accepted --- 12, 2017; Online --- 12, 2017)**

---

## Abstract

The structural analysis of an infinite unsymmetric laminated composite Timoshenko beam over Pasternak viscoelastic foundation under moving load is studied. The beam is subjected to a travelling concentrated load. Closed form steady state solutions, based on the first-order shear deformation theory (FSDT) are developed. In this analysis, the effect of bend-twist coupling is also evaluated. Selecting of an appropriate displacement field for deflection of the composite beam and using the principle of total minimum potential energy, the governing differential equations of motion are obtained and solved using complex infinite Fourier transformation method. The dynamic response of unsymmetric angle-ply laminated beam under moving load has been compared with existing results in the literature and a very good agreement is observed. The results for variation of the deflection, bending moment, shear force and bending stress are presented. In addition, the influences of the stiffness, shear layer viscosity of foundation, velocity of the moving load and also different thicknesses of the beam on the structural response are studied.

**Keywords:** First shear deformation theory; Unsymmetric; Composite beam; Pasternak viscoelastic foundation; Moving load

---

## 1- Introduction

In modern industrialized world as time goes on heavy beams of simple materials are gradually being substituted by light and stronger composite beams. Therefore, the composite beams are often considered as an important element of structures. Structures such as railroads, overhead cranes and bridges are always under the action of dynamic moving loads. Therefore, the analysis of a laminated

composite beam under moving loads may find many practical applications and is of valuable interest in engineering designs.

Many researchers have been performed on dynamic response of the infinite beams resting on various elastic and viscoelastic foundation. Duffy [1] examined vibrations that arised when a moving, vibrating load passes over an infinite railroad track lying on a Winkler foundation. Cai, et al. [2] described an exact method for

investigating the dynamic response of an infinite uniform beam resting on periodic roller supports and subjected to a moving force. Mackertich [3] carried out an analysis of the problem of vibrations of an infinite beam on elastic foundation excited by a moving and vibrating mass. Nguyen and Duhamel [4] presented a numerical approach to the stationary solution of infinite Euler–Bernoulli beams posed on Winkler foundations under moving harmonic loads. Patil [5] determined the resonant frequency of the railroad track by modeling the track as a beam on a massless Winkler Foundation. Uzzal, et al. [6] performed the dynamic response of an Euler–Bernoulli beam supported on two-parameter Pasternak foundation subjected to moving load as well as moving mass. Ding, et al. [7] investigated the dynamic response of infinite Timoshenko beams supported by nonlinear viscoelastic foundations subjected to a moving concentrated force. Mallik, et al. [8] described the steady-state response of a uniform beam placed on an elastic foundation and subjected to a concentrated load moving with a constant speed. Lu and Xuejun [9] performed dynamic analysis of infinite beam under a moving line load with uniform velocity. Kerr [10] showed the advantages of using Pasternak model over the other models. He also further enhanced the elastic model of Pasternak to model viscoelastic foundation.

Chen, et al. [11] established the dynamic stiffness matrix of an infinite or semi-finite Timoshenko beam under harmonic moving load on viscoelastic foundation. Steady state response of a beam on a viscoelastic foundation subjected to harmonic moving load carried out by Sun [12]. He used Fourier transform to solve the problem. Verichev and Metrikine [13] studied the

stability of vibration of a bogie uniformly moving along a Timoshenko beam on a viscoelastic foundation. Liu and Li [14] presented an effective numerical method for solving elastic wave propagation problems in an infinite Timoshenko beam on viscoelastic foundation in time domain. Kargarnovin and Younesian [15] studied the response of a Timoshenko beam with uniform cross-section and infinite length supported by a generalized Pasternak-type viscoelastic foundation subjected to an arbitrary distributed harmonic moving load. The solution of equations of motion resulted in, the distribution of deflection, bending moment and shear force along the beam length. Also, Kargarnovin, et al. [16] studied response of infinite beams supported by nonlinear viscoelastic foundations subjected to harmonic moving loads. They carried out a parametric study and influences of the load speed and frequency on the beam responses investigated. Muscolino and Palmeri [17] studied dynamic response of elastic beams resting on viscoelastically damped foundation under moving oscillators. They used Maxwell model to represent the viscoelastic behavior of a dissipative elastomeric pad. Çalım [18] analyzed dynamic behavior of beams on Pasternak viscoelastic foundation subjected to time-dependent loads. Although dynamic response of beams on viscoelastic foundation is a widely studied topic, there are only few studies that exist in the literature pertaining to the analysis of composite beams on viscoelastic foundation under moving loads.

The composite material for a specific application usually requires the utilization of angle-ply and unsymmetric laminates. Therefore, in their mechanical response can be seen bend-stretch, shear-stretch and

bend-twist coupling effects. Kadivar and Mohebpoor [19] analyzed free vibration of the composite beams and the coupling generated due to bend-twist phenomenon over non-cross-ply laminated composite beam. Rezvani and Khorramabadi [20] carried out dynamic analysis of an infinite Timoshenko beam made of a symmetric laminated composite located on a generalized Pasternak viscoelastic foundation. Later, Rezvani, et al. [21] studied the response of an infinite Timoshenko composite beam subjected to a harmonic moving load based on the third order shear deformation theory (TSDT). They investigated the effects of two types of composite materials with symmetric cross-ply laminates over the beam response. In this paper, the structural analysis of an infinite unsymmetric laminated composite beam on the generalized Pasternak viscoelastic foundation subjected to a concentrated moving load is performed based on the first-order shear deformation theory. After verification of the solution method, the steady-state response of the beam is obtained analytically. In addition, deflection, bending moment, shear force and bending stress are calculated analytically along the beam span in terms of the distance from the position of the moving load. Finally, the effects of the stiffness, shear layer viscosity coefficient of foundation, velocity of moving load and

different thicknesses of the beam on the structural response are investigated.

## 2- Governing Differential Equations of the FSDT

A laminated composite beam with infinite length, a number of layers  $N$ , width of  $b$  and thickness  $h$  is considered. Each lamina is made of an unidirectional reinforced-fiber with the same thickness and the orientations of the layer are unsymmetric. The coordinate system placed at the mid-plane of the laminate as shown in Fig. 1.

Based on the first shear deformation theory (FSDT) and unsymmetric laminated composite beam, the displacements field is [22]:

$$\begin{aligned} U(x, y, z, t) &= z \psi_x(x, t) \\ V(x, y, z, t) &= z \phi_y(x, t) \\ W(x, y, z, t) &= w(x, t) \end{aligned} \quad (1)$$

Where  $U$ ,  $V$  and  $W$  are the beam's displacement components and  $w(x, t)$ ,  $\psi_x(x, t)$  and  $\phi_y(x, t)$  are the beam's deflection, rotational angle due to the bending and rotational angle due to torsion, respectively. Fig. 2 depicts the generalized Pasternak viscoelastic foundation with a viscous shear layer. The transferred forces and moments from the foundation the beam can be calculated as [21]:

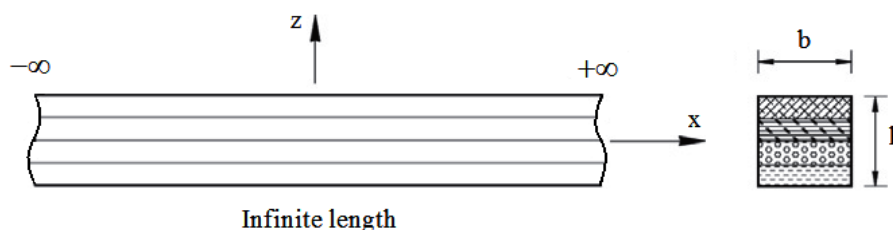


Fig. 1 A schematic of generally laminated composite beam

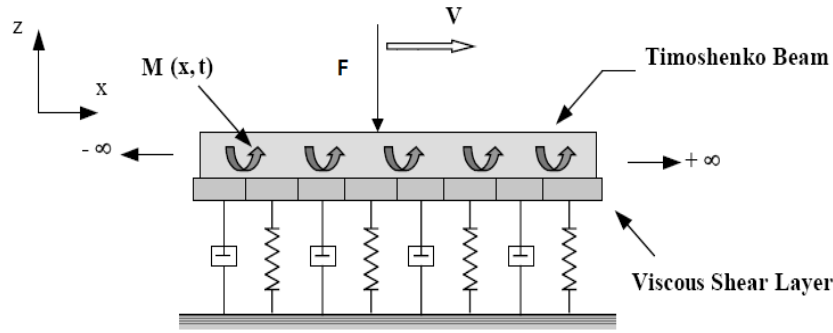


Fig. 2 Extended Pasternak viscoelastic foundation with viscous shear layers

$$\begin{aligned}\tilde{M}_1(x,t) &= -k_\psi \psi_x(x,t) - \eta_\psi \frac{\partial \psi_x(x,t)}{\partial t} \\ \tilde{M}_2(x,t) &= -k_\phi \phi_y(x,t) - \eta_\phi \frac{\partial \phi_y(x,t)}{\partial t} \\ q(x,t) &= -k w(x,t) - \eta \frac{\partial w(x,t)}{\partial t} + \mu \frac{\partial^3 w(x,t)}{\partial t \partial x^2}\end{aligned}\quad (2)$$

Which  $q(x,t)$ ,  $\tilde{M}_1(x,t)$ , and  $\tilde{M}_2(x,t)$  are the foundation excited force, bending moment and torsional moment per unit length of the beam, respectively. Also  $k_\psi$  and  $\eta_\psi$  are the foundation rocking stiffness and damping coefficients,  $k_\phi$  and

$\eta_\phi$  are the foundation torsional stiffness and damping coefficients,  $k$  and  $\eta$  are the foundation normal stiffness and damping coefficients, and  $\mu$  is the foundation shear viscosity coefficient. By applying the total minimum potential energy theorem [23], governing differential equations for the dynamic behavior of the unsymmetric composite laminated beam over Pasternak viscoelastic foundation is found as:

$$b \frac{\partial}{\partial x} [D_{11} \frac{\partial \psi_x}{\partial x}] + b \frac{\partial}{\partial x} [D_{16} \frac{\partial \phi_y}{\partial x}] - b K^2 [A_{45} \phi_y + A_{55} (\psi_x + \frac{\partial w}{\partial x})] - k_\psi \psi_x - \eta_\psi \frac{\partial \psi_x}{\partial t} = b I_2 \frac{\partial^2 \psi_x}{\partial t^2} \quad (3)$$

$$b \frac{\partial}{\partial x} (D_{16} \frac{\partial \psi_x}{\partial x} + D_{66} \frac{\partial \phi_y}{\partial x}) - b K^2 [A_{44} \phi_y + A_{45} (\psi_x + \frac{\partial w}{\partial x})] - k_\phi \phi_y - \eta_\phi \frac{\partial \phi_y}{\partial t} = b I_2 \frac{\partial^2 \phi_y}{\partial t^2} \quad (4)$$

$$b K^2 [A_{45} \frac{\partial \phi_y}{\partial x} + A_{55} (\frac{\partial \psi_x}{\partial x} + \frac{\partial^2 w}{\partial x^2})] + p(x,t) - k w - \eta \frac{\partial w}{\partial t} + \mu \frac{\partial^3 w}{\partial t \partial x^2} = b I_0 \frac{\partial^2 w}{\partial t^2} \quad (5)$$

Which  $K^2$ ,  $b$  and  $p(x,t)$  represent the correction factor for the shear force, width of the beam and moving load, respectively.  $I_0$  and  $I_2$  are the zero and 2<sup>nd</sup>-order moment of inertia such as:

$$\begin{aligned}I_0 &= \int_{-h/2}^{h/2} \rho dz \\ I_2 &= \int_{-h/2}^{h/2} \rho z^2 dz\end{aligned}\quad (6)$$

Which  $\rho$  as the density of the composite beam,  $A_{ij}$  and  $D_{ij}$  are the components of the extensional and bending stiffness matrices which are given as [23]:

$$A_{ij} = \sum_{k=1}^N \bar{Q}_{ij}^{(k)} \int_{z_k}^{z_{k+1}} dz = \sum_{k=1}^N \bar{Q}_{ij}^{(k)} t_k \quad (i, j = 4, 5) \quad (7)$$

$$D_{ij} = \sum_{k=1}^N \bar{Q}_{ij}^{(k)} \left( t_k \frac{z_k^2}{2} + \frac{t_k^3}{12} \right) \quad (i, j = 1, 2, 6) \quad (8)$$

The  $\bar{Q}_{ij}^{(k)}$  represents the reduced transformed stiffness of the  $k^{th}$  layer which are calculated as [23]:

$$\begin{aligned} \bar{Q}_{11} &= m^4 Q_{11} + (2Q_{12} + 4Q_{66})m^2 n^2 \\ &\quad + n^4 Q_{22} \\ \bar{Q}_{12} &= (Q_{11} + Q_{22} - 4Q_{66})m^2 n^2 \\ &\quad + (m^4 + n^4)Q_{12} \\ \bar{Q}_{22} &= n^4 Q_{11} + (2Q_{12} + 4Q_{66})m^2 n^2 \\ &\quad + m^4 Q_{22} \\ \bar{Q}_{16} &= (Q_{11} - Q_{12} - 2Q_{66})m^3 n \\ &\quad + (Q_{12} - Q_{22} + 2Q_{66})n^3 m \\ \bar{Q}_{26} &= (Q_{11} - Q_{12} - 2Q_{66})mn^3 \\ &\quad + (Q_{12} - Q_{22} + 2Q_{66})nm^3 \\ \bar{Q}_{66} &= (Q_{11} + Q_{22} - 2Q_{12} - 2Q_{66})m^2 n^2 \\ &\quad + Q_{66}(n^4 + m^4) \\ \bar{Q}_{44} &= m^2 Q_{44} + n^2 Q_{55} \\ \bar{Q}_{45} &= (Q_{55} - Q_{44})mn \\ \bar{Q}_{55} &= m^2 Q_{55} + n^2 Q_{44} \end{aligned} \quad (9)$$

Which  $m = \cos\theta$ ,  $n = \sin\theta$  and  $Q_{ij}$  are known in terms of the engineering constants and can be written as [23]:

$$\begin{aligned} Q_{11} &= \frac{E_1}{1 - \nu_{12}\nu_{21}} \\ Q_{12} &= \frac{\nu_{21}E_1}{1 - \nu_{12}\nu_{21}} = \frac{\nu_{12}E_2}{1 - \nu_{12}\nu_{21}} \\ Q_{22} &= \frac{E_2}{1 - \nu_{12}\nu_{21}} \\ Q_{55} &= G_{13} \\ Q_{44} &= G_{23} \\ Q_{66} &= G_{12} \end{aligned} \quad (10)$$

In order to calculate the beam steady-state response, a new parameter  $s$  which represents the position of the moving load with respect to the  $x$  direction, is defined as follows:

$$s = x - vt \quad (11)$$

After implementing the following differentiation chain rules:

$$\begin{aligned} \frac{\partial^3}{\partial t \partial x^2} (f(x, t)) &= -v \frac{d^3}{ds^3} (f(s)) \\ \frac{\partial^2}{\partial t^2} (f(x, t)) &= v^2 \frac{d^2}{ds^2} (f(s)) \\ \frac{\partial}{\partial t} (f(x, t)) &= -v \frac{d}{ds} (f(s)) \\ \frac{\partial^2}{\partial x^2} (f(x, t)) &= \frac{d^2}{ds^2} (f(s)) \\ \frac{\partial}{\partial x} (f(x, t)) &= \frac{d}{ds} (f(s)) \end{aligned} \quad (12)$$

On Eqs. (3-5), one can get:

$$\begin{aligned} C_1 \frac{d^2 \psi_x}{ds^2} + C_2 \frac{d^2 \phi_y}{ds^2} + C_3 \psi_x + C_4 \phi_y \\ + C_5 \frac{d \psi_x}{ds} + C_6 \frac{d \phi_y}{ds} = 0 \end{aligned} \quad (13)$$

$$C_7 \frac{d^2 \psi_x}{ds^2} + C_8 \frac{d^2 \phi_y}{ds^2} + C_9 \psi_x + C_{10} \phi_y + C_{11} \frac{d \phi_y}{ds} + C_{12} \frac{dw}{ds} = 0$$

$$C_{13} \frac{d^3 w}{ds^3} + C_{14} \frac{d^2 w}{ds^2} + C_{15} \frac{dw}{ds} + C_{16} w + C_{17} \frac{d \phi_y}{ds} + C_{18} \frac{d \psi_x}{ds} = F(s)$$

The constant coefficients of  $C_1$  to  $C_{18}$  are given in appendix A.

### 3- Solution of Governing Differential Equations

$$\psi_x(q) = \frac{q(i\tilde{B}_1 q^2 + \tilde{B}_2 q + i\tilde{B}_3)F(q)}{i\tilde{B}_{12} q^7 + \tilde{B}_{13} q^6 + i\tilde{B}_{14} q^5 + \tilde{B}_{15} q^4 + i\tilde{B}_{16} q^3 + \tilde{B}_{17} q^2 + i\tilde{B}_{18} q + \tilde{B}_{19}}$$

$$\phi_y(q) = \frac{q(i\tilde{B}_4 q^2 + \tilde{B}_5 q + i\tilde{B}_6)F(q)}{i\tilde{B}_{12} q^7 + \tilde{B}_{13} q^6 + i\tilde{B}_{14} q^5 + \tilde{B}_{15} q^4 + i\tilde{B}_{16} q^3 + \tilde{B}_{17} q^2 + i\tilde{B}_{18} q + \tilde{B}_{19}}$$

$$w(q) = \frac{(\tilde{B}_7 q^4 + i\tilde{B}_8 q^3 + \tilde{B}_9 q^2 + i\tilde{B}_{10} q + \tilde{B}_{11})F(q)}{i\tilde{B}_{12} q^7 + \tilde{B}_{13} q^6 + i\tilde{B}_{14} q^5 + \tilde{B}_{15} q^4 + i\tilde{B}_{16} q^3 + \tilde{B}_{17} q^2 + i\tilde{B}_{18} q + \tilde{B}_{19}}$$

Which the coefficients of  $\tilde{B}_1$  to  $\tilde{B}_{19}$  are given in Appendix B. By performing the

$$\psi_x(s) = \frac{1}{2\pi} \int_{-\infty}^{+\infty} \frac{q(i\tilde{B}_1 q^2 + \tilde{B}_2 q + i\tilde{B}_3)F(q)dq}{i\tilde{B}_{12} q^7 + \tilde{B}_{13} q^6 + i\tilde{B}_{14} q^5 + \tilde{B}_{15} q^4 + i\tilde{B}_{16} q^3 + \tilde{B}_{17} q^2 + i\tilde{B}_{18} q + \tilde{B}_{19}}$$

$$\phi_y(s) = \frac{1}{2\pi} \int_{-\infty}^{+\infty} \frac{q(i\tilde{B}_4 q^2 + \tilde{B}_5 q + i\tilde{B}_6)F(q)dq}{i\tilde{B}_{12} q^7 + \tilde{B}_{13} q^6 + i\tilde{B}_{14} q^5 + \tilde{B}_{15} q^4 + i\tilde{B}_{16} q^3 + \tilde{B}_{17} q^2 + i\tilde{B}_{18} q + \tilde{B}_{19}}$$

$$w(s) = \frac{1}{2\pi} \int_{-\infty}^{+\infty} \frac{(\tilde{B}_7 q^4 + i\tilde{B}_8 q^3 + \tilde{B}_9 q^2 + i\tilde{B}_{10} q + \tilde{B}_{11})F(q)dq}{i\tilde{B}_{12} q^7 + \tilde{B}_{13} q^6 + i\tilde{B}_{14} q^5 + \tilde{B}_{15} q^4 + i\tilde{B}_{16} q^3 + \tilde{B}_{17} q^2 + i\tilde{B}_{18} q + \tilde{B}_{19}}$$

### 4-Results and Discussion

In this section, numerical results are presented for an unsymmetrical laminated

To facilitate solution of motion's differential equations the complex Fourier Transform and its inverse defined as [24]:

$$F(q) = \int_{-\infty}^{+\infty} f(s)e^{-isq} ds$$

$$f(s) = \frac{1}{2\pi} \int_{-\infty}^{+\infty} F(q)e^{isq} dq$$

After implementing the Fourier transform on Eq. (13), the complex Fourier Transforms of  $w(q)$ ,  $\psi_x(q)$  and  $\phi_y(q)$  are obtained as:

inverse Fourier transform on Eq. (15),  $\psi_x(s)$ ,  $\phi_y(s)$  and  $w(s)$  become:

composite beam (0/45/-45/90). In this example we will demonstrate the

importance of the bend-twist coupling term in such beam. Table 1 shows the different property details of the T300/5208

composite beam [23] and Pasternak viscoelastic foundation [21].

Table 1 Different property details of the composite T300/5208 beam and Pasternak viscoelastic foundation [21, 23]

Geometrical data for the composite layers	Mechanical properties of composite beam	Mechanical properties of Pasternak viscoelastic foundation
Number of layers ( $N = 4$ )	$\rho = 1540 \text{ kg / m}^3$	$k_{\psi} = 13.8 \text{ MN}$
Width the beam ( $b = 5 \text{ cm}$ )	$E_1 = 132 \text{ Gpa}$	$\eta_{\psi} = 5520 \text{ N .s}$
The thickness of the beam ( $h = 10 \text{ cm}$ )	$E_2 = 10.8 \text{ Gpa}$	$k_{\phi} = 13.8 \text{ MN}$
Angle-ply laminated beam ( $0 / 45 / -45 / 90$ )	$G_{12} = 5.65 \text{ Gpa}$	$\eta_{\phi} = 5520 \text{ N .s}$
Correction factor for shear force $K = 5 / 6$	$G_{13} = G_{23} = 3.38 \text{ Gpa}$	$\mu = 69 \text{ kN .s}$
Magnitude load velocity $v = 40 \text{ m / s}$	$\nu_{12} = 0.24$	$k = 69 \text{ Mpa}$
Magnitude of the moving load $F(s) = 144600 \delta(s)$	$\nu_{13} = \nu_{23} = 0.59$	$\eta = 138 \text{ kN .s / m}^2$

In this study, the results are compared with the analytical results an isotropic Euler-Bernoulli beam under moving load obtained by Fryba [25]. For this purpose, the shear viscosity coefficient, foundation rocking stiffness, damping coefficients and normal damping coefficient in our analysis are neglected. By setting these coefficients equal to zero in Eqs. (3) and (5), one deals with a beam supported by a Winkler elastic foundation.

$$b \frac{\partial}{\partial x} [D_{11} \frac{\partial \psi_x}{\partial x}] - b K^2 A_{55} (\psi_x + \frac{\partial w}{\partial x}) = b I_2 \frac{\partial^2 \psi_x}{\partial t^2} \quad (17)$$

$$b \frac{\partial}{\partial x} [K^2 A_{55} (\psi_x + \frac{\partial w}{\partial x})] + p(x, t) - k w = b I_0 \frac{\partial^2 w}{\partial t^2} \quad (18)$$

By substituting  $\psi_x = -\frac{\partial w}{\partial x}$ ,  $D_{11} = EI$ ,

$$A_{55} = GA, I_2 = \rho I, I_0 = \rho A \text{ and } K^2 = k^*$$

and neglect the effect of rotary inertia in Eqs. (17) and (18), the governing differential equations for the dynamic behavior of isotropic Euler-Bernoulli beam over elastic foundation is found as:

$$EI \frac{\partial^4 w}{\partial x^4} + \rho A \frac{\partial^2 w}{\partial x^2} + k w = p(x, t) \quad (18)$$

This equation is exactly the same as the one given in the literature for the dynamic response of an isotropic Euler-Bernoulli beam supported by a Winkler elastic foundation under the motion of a traveling load [25]. After implementing the Fourier transform on Eq. (19), primarily the displacement and subsequently the bending moment and shear force can be calculated. The variation of  $w$ ,  $M_x$  and  $Q_x$  versus  $s$  are plotted in Fig. 3. It has to be mentioned that the plots in the Fig. 3 are similar to those presented in Ref [16].

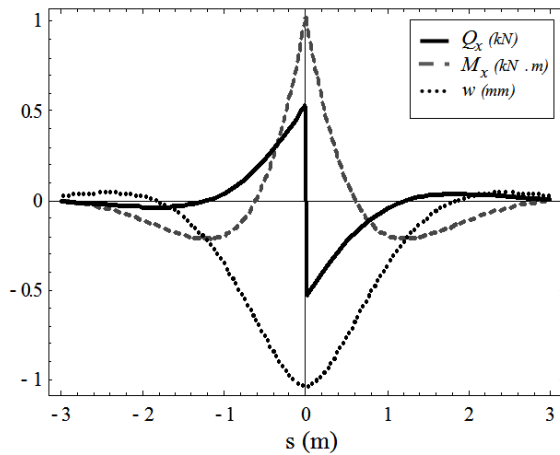


Fig. 3 Deflection, bending moment and shear force for isotropic Euler-Bernoulli beam over a Winkler elastic foundation [25]

#### 4-1-Comparison between symmetric and unsymmetric laminated composite beam

In this section, by using the data of given in Table 1, the values of  $w$ ,  $\psi_x$  and  $\phi_y$  are solved for two cases of the symmetric (0/90/90/0) and the unsymmetric (0/45/-45/90) configurations [19]. Then, by employing Eqs. (15-17), the shear force, bending moment and bending stress are accordingly obtained. The results for deflection, shear force, bending moment and bending stress distribution of symmetric and unsymmetric composite laminated beam are presented vs.  $s$ , the distance from the position of the moving load in Figs. (4-7). As it is evident from Fig. 4, there is almost no difference between the deflection of symmetric and unsymmetric laminated composite beam.

The variation of the shear force of symmetric and unsymmetric laminated composite beam is shown in Fig.5. As shown in this figure, except point around  $s = 0$ , interval the shear force values for two beams are almost the same. Moreover, there is a sign change for the shear force for points before and after the point of load exertion

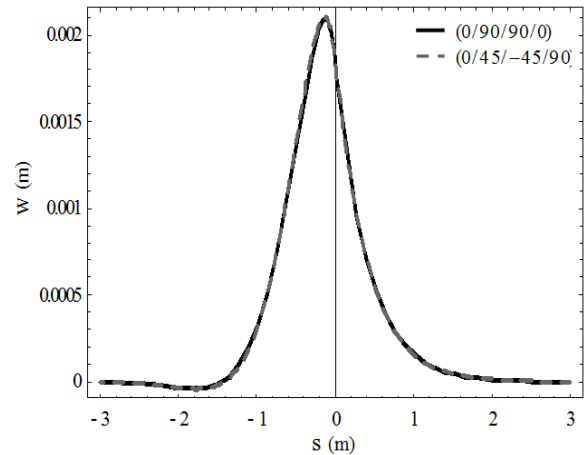


Fig. 4 Comparison of deflection variation for symmetric and unsymmetric composite beam

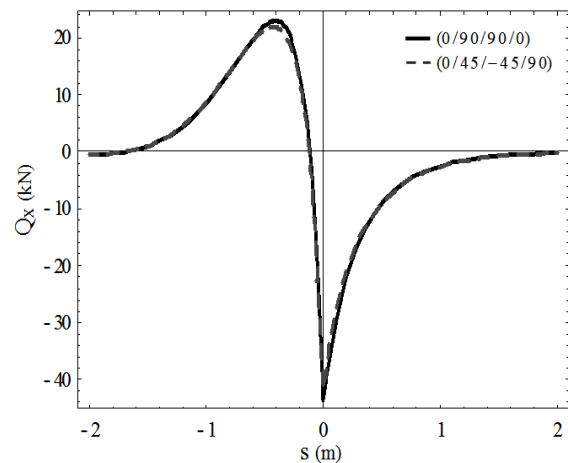


Fig. 5 Comparison of shear force distribution between symmetric and unsymmetric composite beam

Figure 6 shows the bending moment distribution for symmetric and unsymmetric laminated composite beam. Contrary to two previous cases, this figure depicts a clear difference between load carrying capacity of unsymmetric laminate composite beam and symmetric one. However, in both beams the maximum bending moment is located near to the point where the point load is applied. It can also be seen that the magnitude of the bending moment in the unsymmetric laminated composite beam is less than the symmetric one.

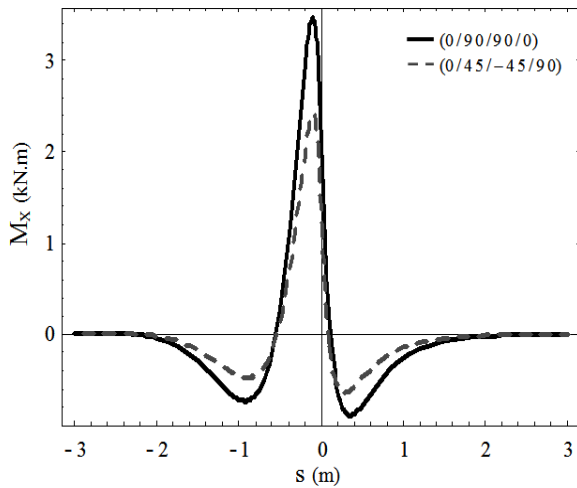


Fig. 6 Bending moment vs.  $s$  distribution of a symmetric and unsymmetric composite beam

Having the bending moment distribution, one can easily obtain the bending stress,  $\sigma_x$  for symmetric and unsymmetric laminated composite beam. Fig.7 illustrates the bending stress distribution on the upper layer. Having the bending moment distribution, one can easily obtain the bending stress,  $\sigma_x$  for symmetric and unsymmetric laminated composite beam. Fig.7 illustrates the bending stress distribution on the upper layer.

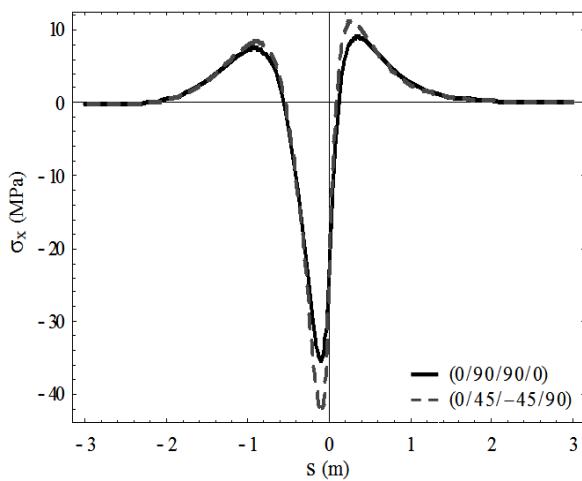


Fig. 7 Bending stress vs.  $s$  distribution of a symmetric and unsymmetric composite beam for the upper layer

#### 4-2-Effects of different parameters on the beam deflection

The maximum value of deflection of an unsymmetric laminated composite beam with varying of the foundation normal stiffness, foundation viscosity and the moving load velocity is shown in Fig 8. As seen in this figure, by increasing the foundation normal stiffness coefficient, the maximum value of deflection decreases and it moves towards the point where the load is applied i.e.  $s = 0$ . Also, by increasing the foundation viscosity coefficient and the moving load velocity, the maximum value of deflection decreases and it moves further away from the point where the load is applied ( $s = 0$ ).

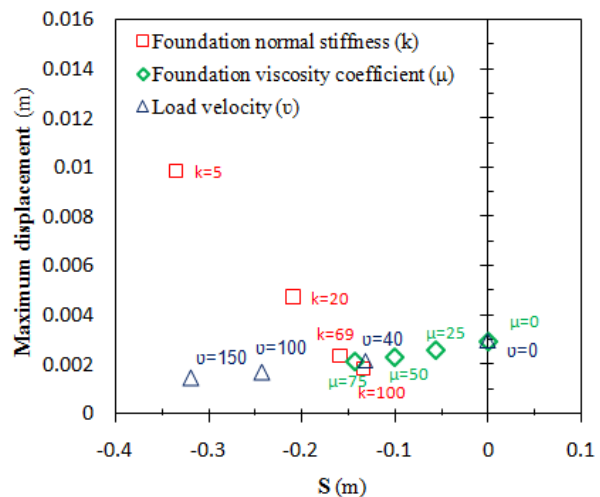


Fig. 8 Effects of different parameters on the maximum value of the deflection

#### 4-3-Effects of different parameters on the shear force

The maximum value of the shear force of an unsymmetric laminated composite beam with varying of the foundation normal stiffness, foundation viscosity and the moving load velocity is shown in Fig 9. As illustrated in this figure, the maximum value of the shear force takes place right at the point where the load is exerted i.e.  $s = 0$ . Moreover, as foundation normal

stiffness coefficient, foundation viscosity coefficient and the moving load velocity increases, the maximum value of the shear force decreases

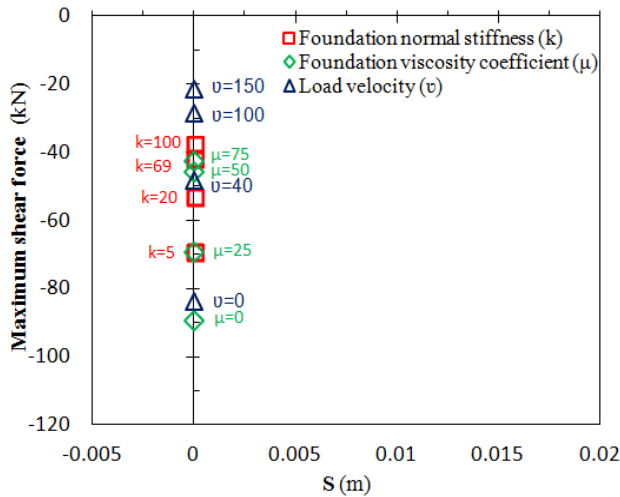


Fig. 9 Effects of different parameters on the maximum value of the shear force

#### 4-4-Effects of different parameters on the bending moment

Figure 10 shows the effects of different parameters such as the foundation normal stiffness coefficient, foundation viscosity coefficient and the moving load velocity on the maximum value of the bending moment of an unsymmetric laminated composite beam. As observed, by increasing the foundation normal stiffness coefficient, the maximum value of bending moment moves closer to the point where the load is applied ( $s=0$ ). Whereas, by increasing the foundation viscosity coefficient and the moving load velocity, the maximum value of the bending moment decreases and the point of maximum bending moment moves further away from the load exertion point ( $s=0$ ). Also, when the foundation shear viscosity coefficient and the moving load velocity are zero, the bending moment diagram has

a maximum value at the point where the moving load is applied ( $s=0$ )

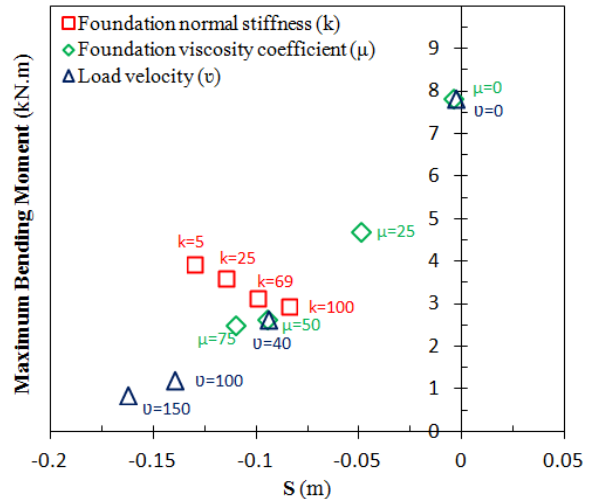


Fig. 10 Effects of different parameters on the maximum value of the bending moment

#### 4-5-Effects of different parameters on the bending stress distribution

It is clear that in the laminated composite beam the linear trend of normal stress variation due to the bending moment does not change in each layer. Therefore, to investigate the effects of different parameters on the normal stress distribution of the entire cross section, analysis was conducted only on the upper layer of the beam. Figure 11 shows the effects of different parameters such as the foundation normal stiffness coefficient, foundation viscosity coefficient and the moving load velocity on  $\sigma_x$  distribution of the central line of upper layer of an unsymmetric laminated composite beam. As illustrated in the figure, by increasing the value of  $k$ , the maximum value of the stress decreases and it moves closer to the point where the load is applied. As seen, when the foundation shear viscosity coefficient and the moving load velocity

are zero, the value of stress  $\sigma_x$  are maximum at the moving load exertion point. By increasing the foundation viscosity coefficient and the moving load velocity, this maximum point moves behind of the load exertion point and the value of stress  $\sigma_x$  decreases.

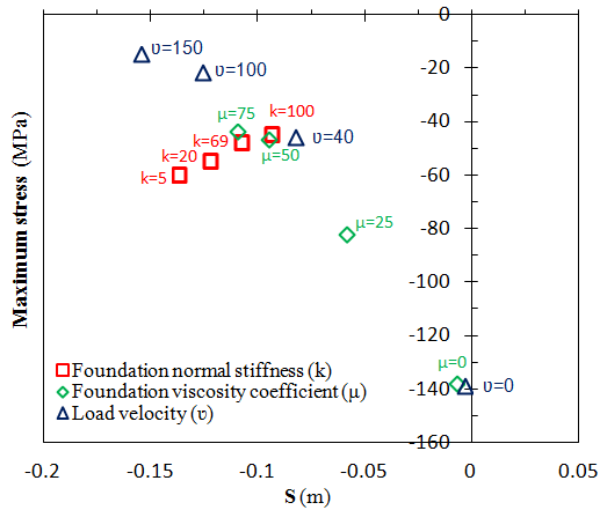


Fig. 11 Effects of different parameters on the  $\sigma_x$  distribution

### 5-Conclusions

In this study, the behaviour of an unsymmetric laminated composite beam over Pasternak viscoelastic foundation under travelling concentrated load was analyzed. For this purpose, by employing the first order shear deformation theory and using the principle of total minimum potential energy, the governing differential equations of motion were obtained. The complex infinite Fourier transformation method applied as well and the obtained analytically parameter values of deflection, bending moment, shear force and the bending stress. Based on this analysis the following were concluded:

1. By increasing the foundation normal stiffness coefficients, the maximum value of beam deflection, bending moment and

stress decreased and the maximum value of deflection was approached closer to the moving load exertion point.

2. By increasing the foundation viscosity coefficient and the moving load velocity, the maximum value of deflection, bending moment and the stress decreased and it was moved further away from the point where the load was applied.

3. The maximum value of the bending moment and the stress occurred when the foundation viscosity coefficient and the moving load velocity were zero and it takes placed right at the point where the load was exerted i.e.  $s = 0$ .

4. By increasing the foundation normal stiffness coefficient, foundation viscosity coefficient and the moving load velocity, the maximum value of the shear force decreased and it takes placed right at the point where the load was exerted i.e.  $s = 0$ .

All of the obtained results may be useful for design purposes and a better understanding of the behavior of the structural systems of railways under moving loads.

### Appendix

#### Appendix A

Parameters of Eq. (13)

$$\begin{aligned}
 C_1 &= b D_{11} - b I_2 v^2 & C_{10} &= -b K^2 A_{44} - k_\phi \\
 C_2 &= b D_{16} & C_{11} &= \eta \phi v \\
 C_3 &= -b K^2 A_{55} - k_\psi & C_{12} &= -b K^2 A_{45} \\
 C_4 &= -b K^2 A_{45} & C_{13} &= \mu v \\
 C_5 &= \eta_\psi v & C_{14} &= -b K^2 A_{55} + b I_0 v^2 \\
 C_6 &= -b K^2 A_{55} & C_{15} &= -\eta v \\
 C_7 &= b D_{16} & C_{16} &= k \\
 C_8 &= b D_{66} - b I_2 v^2 & C_{17} &= -b K^2 A_{45} \\
 C_9 &= -b K^2 A_{45} & C_{18} &= -b K^2 A_{55}
 \end{aligned}$$

## Appendix B

Parameters of Eq. (15)

$$\tilde{B}_1 = C_2 C_{12} - C_6 C_7 - C_6 C_8$$

$$\tilde{B}_2 = -C_6 C_{11}$$

$$\tilde{B}_3 = C_6 C_9 - C_4 C_{12} + C_6 C_{10}$$

$$\tilde{B}_4 = -C_1 C_{12}$$

$$\tilde{B}_5 = -C_{12} C_5$$

$$\tilde{B}_6 = C_{12} C_3$$

$$\tilde{B}_7 = -C_1 C_8 - C_1 C_7$$

$$\tilde{B}_8 = C_8 C_5 + C_7 C_5 + C_1 C_{11}$$

$$\tilde{B}_9 = C_5 C_{11} + C_1 C_{10} + C_1 C_9 + C_3 C_8 + C_3 C_7$$

$$\tilde{B}_{10} = -C_{10} C_5 - C_9 C_5 - C_3 C_{11}$$

$$\tilde{B}_{11} = -C_{10} C_3 - C_3 C_9$$

$$\tilde{B}_{12} = -C_1 C_{13} C_7 + C_1 C_{13} C_8$$

$$\tilde{B}_{13} = C_5 C_{13} C_8 + C_1 C_{14} C_8 + C_1 C_{13} C_{11} + C_5 C_{13} C_7 + C_1 C_{14} C_7$$

$$\tilde{B}_{14} = -C_3 C_{13} C_8 - C_3 C_{13} C_7 - C_1 C_{13} C_9 - C_1 C_{15} C_8 - C_5 C_{13} C_{11} - C_5 C_{14} C_8 - C_5 C_{14} C_7 - C_1 C_{14} C_{11} - C_1 C_{15} C_7 - C_1 C_{13} C_{10}$$

$$\tilde{B}_{15} = -C_5 C_{13} C_{10} - C_1 C_{16} C_7 - C_1 C_{15} C_{11} - C_1 C_{16} C_8 - C_3 C_{13} C_{11} - C_3 C_{14} C_8 + C_1 C_{17} C_{12} - C_3 C_{14} C_7$$

$$- C_2 C_{12} C_{18} + C_6 C_7 C_{18} - C_1 C_{14} C_{10} + C_6 C_8 C_{18} - C_5 C_{13} C_9 - C_5 C_{14} C_{11} - C_5 C_{15} C_8 - C_5 C_{15} C_7 - C_1 C_{14} C_9$$

$$\tilde{B}_{16} = C_3 C_{14} C_{11} + C_3 C_{15} C_8 + C_3 C_{15} C_7 + C_5 C_{15} C_{11} + C_5 C_{16} C_8 + C_5 C_{14} C_9 + C_5 C_{16} C_7 - C_5 C_{17} C_{12}$$

$$+ C_3 C_{13} C_{10} + C_3 C_{13} C_9 + C_1 C_{15} C_{10} + C_1 C_{16} C_{11} + C_5 C_{14} C_{10} + C_1 C_{15} C_9 - C_6 C_{11} C_{18}$$

$$\tilde{B}_{17} = C_5 C_{15} C_9 + C_5 C_{16} C_{11} + C_3 C_{16} C_7 + C_3 C_{16} C_8 - C_3 C_{17} C_{12} + C_1 C_{16} C_{10} + C_1 C_{16} C_9$$

$$+ C_3 C_{14} C_{10} + C_3 C_{14} C_9 + C_3 C_{13} C_{11} - C_6 C_9 C_{18} + C_4 C_{12} C_{18} - C_6 C_{10} C_{18} + C_5 C_{15} C_{10}$$

$$\tilde{B}_{18} = -C_3 C_{15} C_{10} - C_3 C_{15} C_9 - C_3 C_{16} C_{11} - C_5 C_{16} C_{10} - C_5 C_{16} C_9$$

$$\tilde{B}_{19} = -C_3 C_{16} C_9 - C_3 C_{16} C_{10}$$

## References

- [1] D. G. Duffy, "The response of an infinite railroad track to a moving, vibrating mass," *Journal of Applied Mechanics*, vol. 57, pp. 66-73, 1990.
- [2] C. Cai, Y. Cheung, and H. Chan, "Dynamic response of infinite continuous beams subjected to a moving force—an exact method," *Journal of Sound and Vibration*, vol. 123, pp. 461-472, 1988.

- [3] S. Mackertich, "The response of an elastically supported infinite Timoshenko beam to a moving vibrating mass," *The Journal of the Acoustical Society of America*, vol. 101, pp. 337-340, 1997.
- [4] V.-H. Nguyen and D. Duhamel, "Finite element procedures for nonlinear structures in moving coordinates. Part II: Infinite beam under moving harmonic loads," *Computers & Structures*, vol. 86, pp. 2056-2063, 2008.

- [5] S. P. Patil, "Response of infinite railroad track to vibrating mass," *Journal of engineering mechanics*, vol. 114, pp. 688-703, 1988.
- [6] R. U. A. Uzzal, R. B. Bhat, and W. Ahmed, "Dynamic response of a beam subjected to moving load and moving mass supported by Pasternak foundation," *Shock and Vibration*, vol. 19, pp. 205-220, 2012.
- [7] H. Ding, K.-L. Shi, L.-Q. Chen, and S.-P. Yang, "Dynamic response of an infinite Timoshenko beam on a nonlinear viscoelastic foundation to a moving load," *Nonlinear Dynamics*, vol. 73, pp. 285-298, 2013.
- [8] A. Mallik, S. Chandra, and A. B. Singh, "Steady-state response of an elastically supported infinite beam to a moving load," *Journal of Sound and Vibration*, vol. 291, pp. 1148-1169, 2006.
- [9] S. Lu and D. Xuejun, "Dynamic analysis to infinite beam under a moving line load with uniform velocity," *Applied mathematics and mechanics*, vol. 19, pp. 367-373, 1998.
- [10] A. D. Kerr, "Elastic and viscoelastic foundation models," *Journal of Applied Mechanics*, vol. 31, pp. 491-498, 1964.
- [11] Y.-H. Chen, Y.-H. Huang, and C.-T. Shih, "Response of an infinite Timoshenko beam on a viscoelastic foundation to a harmonic moving load," *Journal of Sound and Vibration*, vol. 241, pp. 809-824, 2001.
- [12] L. Sun, "A closed-form solution of a Bernoulli-Euler beam on a viscoelastic foundation under harmonic line loads," *Journal of Sound and vibration*, vol. 242, pp. 619-627, 2001.
- [13] S. Verichev and A. Metrikine, "Instability of a bogie moving on a flexibly supported Timoshenko beam," *Journal of sound and vibration*, vol. 253, pp. 653-668, 2002.
- [14] T. Liu and Q. Li, "Transient elastic wave propagation in an infinite Timoshenko beam on viscoelastic foundation," *International journal of solids and structures*, vol. 40, pp. 3211-3228, 2003.
- [15] M. Kargarnovin and D. Younesian, "Dynamics of Timoshenko beams on Pasternak foundation under moving load," *Mechanics Research Communications*, vol. 31, pp. 713-723, 2004.
- [16] M. Kargarnovin, D. Younesian, D. Thompson, and C. Jones, "Response of beams on nonlinear viscoelastic foundations to harmonic moving loads," *Computers & Structures*, vol. 83, pp. 1865-1877, 2005.
- [17] G. Muscolino and A. Palmeri, "Response of beams resting on viscoelastically damped foundation to moving oscillators," *International Journal of Solids and Structures*, vol. 44, pp. 1317-1336, 2007.
- [18] F. F. Çalım, "Dynamic analysis of beams on viscoelastic foundation," *European Journal of Mechanics-A/Solids*, vol. 28, pp. 469-476, 2009.
- [19] M. Kadivar and S. Mohebpour, "Finite element dynamic analysis of unsymmetric composite laminated beams with shear effect and rotary inertia under the action of moving loads," *Finite elements in Analysis and Design*, vol. 29, pp. 259-273, 1998.
- [20] M. Rezvani and K. M. Khorramabadi, "Dynamic analysis of a composite beam subjected to a moving load," *Proceedings of the Institution of Mechanical Engineers, Part C: Journal of Mechanical Engineering Science*, vol. 223, pp. 1543-1554, 2009.
- [21] M. J. Rezvani, M. H. Kargarnovin, and D. Younesian, "Dynamic analysis of composite beam subjected to harmonic moving load based on the third-order shear deformation theory," *Frontiers of Mechanical Engineering*, vol. 6, pp. 409-418, 2011.
- [22] H. Abramovich and A. Livshits, "Free vibrations of non-symmetric cross-ply laminated composite beams," *Journal of sound and vibration*, vol. 176, pp. 597-612, 1994.

- [23] J. N. Reddy, *Mechanics of laminated composite plates and shells: theory and analysis*: CRC press, 2004.
- [24] A. David Wunsch, "Complex Variables With Applications [M]," ed: Reading, Mass: Addison-Wesley Publishing Company, 1994.
- [25] L. Fryba, *Vibration of solids and structures under moving loads*: Thomas Telford, 1999.